Published in *Kinematic and Physics of Celestial Bodies*, Vol. **17**, N5, p.424-436, 2001

Measurements of horizontal motion of the station Simeiz using VLBI

L. Petrov[1]*, O. Volvach[2], N. Nesterov[2]

1) Code 926, NVI, Inc./NASA Goddard Space Flight Center, Greenbelt, MD 20771 USA
2) Crimean Astrophysical Observatory, RT-22, 98688, Katsively, Crimea, Ukraine

Abstract:

Estimates of the horizontal velocity of the radioastronomical station Simeiz were obtained using VLBI observations made under geodynamics programs during the years 1994-2000. The complete set of 3 million VLBI observations was analyzed, and it was found that the station moves with respect to the Eurasian tectonic plate, considered as rigid, with a rate of 2.8 ± 0.9 *mm/yr in the north-east direction. Possible local systematic effects were thoroughly studied and the reliability of the estimate of uncertainty of the results was evaluated. We investigated stability of the station with respect to local marks and revealed that an inclination of the azimuthal axis of the telescope increases with velocity* $2''.6$ *per year. The estimate of vertical motion of the station, 2.6 ± 3.0 mm/yr, is not statistically significant.*

Introduction

The fundamental geodynamics station “Simeiz-Katsively” is situated on the coast of the Black Sea near the village Simeiz, approximately 20 km west of the city Yalta, in the Ukraine. It consists of two satellite laser ranging stations, a permanent GPS receiver, a sea level gauge and the radiotelescope RT-22 all located within 3 km (Bolotin, et al., 1995), (Tatevian and Shtirberg, 1999). The 22-m radiotelescope owned by the Crimean Astrophysical Observatory participated in the very first intercontinental very long baseline interferometric (VLBI) observations in September 1969 under astrophysical programs (Broderick, et al., 1970). The early narrow-band VLBI observations provided decameter accuracy (Matveenko, et al., 1992) and were not useful for geodynamics applications. The telescope was upgraded in 1994. A Mark 3A data acquisition terminal (Clark, et al., 1985) and a dual-frequency horn were loaned by NASA/GSFC, dual band S/X receivers were supplied by the Institute of Applied Astronomy in Sanct-Petersburg, Russia, a CH-70 hydrogen maser was supplied by the Institute of Space Research in Moscow. Interferometric fringes were obtained in the first test carried out on June 20, 1994. This upgrade enabled the station to join international observing campaigns for both astrophysical and geodynamics programs (Clark, et al., 1995), (Petrov, et al., 1995a).

Regular VLBI observations of extragalactic sources under geodynamics programs are a part of common efforts to maintain the terrestrial and celestial reference frames and to

*e-mail address for offprint requests: pet@leo.gsfc.nasa.gov

monitor Earth orientation parameters. These activities are coordinated by the International VLBI Service for Geodesy and Astrometry (IVS) (Vandenberg, 1999). Analysis of these observations allows us to obtain the estimates of the parameters of models of geophysics (Takahashi, et al., 2000), astrometry (Walter and Sovers, 2000) and gravitational theory (Pyne, et al., 1996).

In this paper we present our study for determination of position and rate of change of the VLBI station Simeiz using the full set of observations since 1994. The method of VLBI proposed by Matveenko (Matveenko, et al., 1965) allows us to reach a precision better than 0.2 mm for station position determination (Hase and Petrov, 1999). However, the actual accuracy is substantially worse since there are factors which systematically affect results of the measurements. These includes instrumental errors caused by an instability of the radioelectronics and by spurious signals of various origin, deficiencies of the geophysical models used in reduction of the observations, displacements of the antenna's reference point with respect to local marks due to deformations.

Investigation of systematic errors allows us to obtain more accurate estimates of the targeted parameters and to get more realistic estimates of their uncertainties. General analysis of the VLBI systematic errors is beyond the scope of the this paper and can be found in (Ray and Corey, 1991), (MacMillan and Ma, 1994), (Takahashi, et al., 2000) and (Petrov, 2000). We consider here only specific local effects, which were discovered during our study. The purpose of our paper is to derive the velocity of the VLBI station Simeiz with respect to other VLBI stations located on the Eurasian plate and to obtain the reliable estimate of its accuracy.

Characteristics of the VLBI network station Simeiz

The radiotelescope RT-22 has a steering parabolic mirror with diameter 22 m and focal length 9 525 mm. The surface has a root mean square accuracy 0.25 mm and effective area 210 m^2 which does not depend on elevation angle. The antenna has an azimuth-elevation mounting with axis offset -1.8 ± 0.2 mm. Working range in azimuth is $[-210°, 210°]$[1] and in elevation $[-1°, 85°]$. The maximum slewing rate is $1\overset{\circ}{.}5$/sec. The control system of the telescope provides accuracy of pointing at the $10''$ level.

The foundation pit of the telescope is 9 meters deep. It has 3 meters of crushed stones and a 6 meters concrete foundation. The height of the elevation axis above the foundation is 14.998 meters. The telescope is located 80 meters from the edge of the Black sea. The reference point of the radiotelescope has IVS name: "CRIMEA", ITRF name: "Simeis", IERS dome number 12337S008 and CDP number 7332.

Low noise receivers at X (3.6 cm) and S (13 cm) bands with a dual-frequency feed have been installed at the prime focus of the antenna. The feed illuminates the main dish of the antenna over the angle of 140° at the level -10 db. The feed may receive both left and right circular polarizations at X band and either left or right circular polarization at S band, although only one polarization can be recorded during observations.

S and X band receivers are constructed using a superheterodyne scheme with FET high frequency amplifiers. A fronted directional coupler and FET amplifiers are cooled to 20 K by a micro-cryogenic, closed cycle system in order to reduce thermal noise. Focusing

[1] Azimuth is counted from north to east in this paper.

fig. 1: System temperature in K versus elevation angle. Experiment 98AUG17XA.

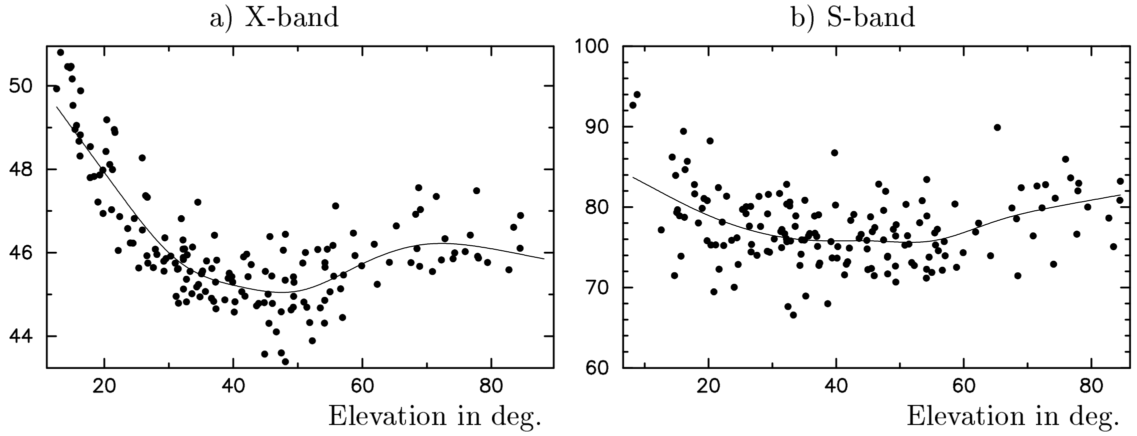

the system and measurements of the system equivalent flux density (SEFD) are made by measuring the power pattern of the antenna from observations of the strongest radio sources Taurus-A, Virgo-A, Cas-A and Cygnus-A before and after each observing session. Typical values of SEFD are 800Jy at X-band and 1200Jy at S-band. System temperature is measured before each observation for diagnostic purposes and for scaling the amplitude of the phase calibration signal. Elevation dependence of the system temperature measured during an experiment is shown in figure 1. Increasing system temperature at the elevations lower than 30° above the horizon is caused by increasing atmospheric depth.

Observations

Data flow follows this scheme:

Schedule center	$\longrightarrow$	Observing Stations	$\longrightarrow$	Correlation center	$\longrightarrow$	Analysis centers	$\longrightarrow$	Data centers

A schedule center prepares an experiment and sends control files to the observing stations by e-mail. The control files define the equipment setup and a timetable of observations of each source. The sequence of the observations is optimized in accordance with the primary objective of the observing session.

The observing station runs a control program "Field system" (Himwich, 2000) which interprets the schedule control file and operates the antenna and the data acquisition terminal. The system is designed to run in automatic mode with minimal human interference. The observing station executes a sequence of two main operations: a) slewing antenna on the source; b) tracking the source and recording the signal at 14 channels with bandwidth 2 MHz in two bands: 8.2–8.6 GHz and 2.2–2.3 MHz during scanning time (typically 60–300 seconds). Upon completion of observing one source the telescope immediately slews to the next source. Usually 30–100 sources, which are more or less uniformly distributed over the sky, are observed. These sources are compact and have flux densities of 0.1–10 Jy. Roughly speaking the antenna spends half of the time slewing and half of the time recording the signal. An observing session lasts for 24 hours without interruption, each station makes 200–500 scans and collects 2–5 Terabits of data, which are recorded on magnetic tapes.

The tapes are sent to one of the correlation centers: Max-Plank Institute for Radioastronomy in Bonn, Haystack observatory in Westford, Massachusetts, or US Naval Observatory in Washington D.C., USA.

The correlation center plays back the tapes from all stations that participated in the session on a specially dedicated supercomputer called a "correlator". The correlator computes the cross-correlation function of the recorded signal. Then for each scan, for each baseline, for each band five basic quantities are calculated: single-band group delay, multiband group delay, delay rate, amplitude and phase of the coherence function and their formal uncertainties. The ionosphere free linear combination of group delays at X and S bands on a baseline referred to a fiducial epoch within a scan is a basic observable which is thereupon referred to as observation. The output from the correlator and post-correlation analysis is sent to the IVS Data Center center via Internet. The data become accessible on-line to public, without restrictions, within minutes after completion of correlation.

The analysis center carries out preliminary processing. This includes resolving group delay ambiguities, rejecting outliers, determining clock model, re-weighting the observations, applying external calibrations and archiving the data. Parameters of a simplified model, including station positions, clock function, atmosphere path delay are obtained by least squares (LSQ). Station performance is evaluated and discovered problems are reported. Then the archived data and the results of the analysis are automatically transmitted to an IVS Data Center. This normally occurs within 24 hours after completion of correlation and within 7–90 days after observations.

Data analysis

All available dual-band geodetic Mark 3 VLBI observations for 21 years, from 1979.59 through 2000.72, were used in this analysis. There were 3 058 sessions, **3 005 651** observations including 36 successful sessions with participation of the station Simeiz. These 36 sessions were from 1994.48 through 2000.36 and contained **19 631** good measurements of group delays.

We used the software CALC/SOLVE for data analysis. Theoretical values of group delay as well as partial derivatives of delay with respect to parameters of the model were computed (Sovers, et al., 1998) and small differences between the observed and calculated values of time delay were formed. Adjustments to parameters of the model were obtained in a single weighted LSQ solution.

The 756 sources and 127 stations participated in the observations were split onto two categories: primary and secondary.

Estimated parameters belong to one of the three groups:

- **global** (over the entire data set): positions and velocities of 43 primary stations; positions of 392 primary sources.
- **local** (over each session): pole coordinates, UT1, UT1 rate, nutation angles; positions of secondary stations and sources, atmosphere gradients for all stations and their rate, station-dependent clocks modeled by 2nd order polynomials, baseline-dependent clock offsets.

- **segmented** (over 0.5–1.0 hours): coefficients of a linear spline for clocks (1 hour segment) and for atmospheric path delay (0.5 hour segment) for each station.

Since the resulting normal matrix is a matrix of incomplete rank, the following constraints on global parameters were imposed in order to resolve singularity: no-net-rotation constraints on global station positions, station velocities, source coordinates; no-net-translation constraints on station positions and velocities. In total, 15 equations of constraint on global parameters were used. The rate of change of atmosphere path delay and clock function between two adjacent segments was constrained to zero with weights reciprocal to 40 psec/hour and $2 \cdot 10^{-14}$ sec/sec respectively.

Special fast algorithms which exploit sparseness of the normal matrix and regularity of its portrait were used for direct solving of the LSQ problem with 1.1 million unknowns.

The station Simeiz was treated as a primary station in solution 1 and therefore its position and velocity was estimated using all data. The overall weighted root mean square (wrms) of postfit residuals of the solution was 25.2 psec with $\chi^2/\mathrm{ndg} = 1.03$, the wrms of the postfit residuals of the observations with station Simeiz was 40.8 psec.

Evaluation of stability of the reference point

The reference point of the antenna is the point of projection of the azimuthal axis on the elevation axis. The coordinates of just this point are determined in analysis of the observations. However, this point may move with respect to the local area where the radiotelescope is located. In order to exclude local motion of the antenna, the coordinates of the reference point with respect to a set of local marks around the telescope were determined by measuring the position of the antenna axes. Two methods were used: analysis of a set of corrections to pointing to the radiosources and direct measurements of the deviation of the azimuthal axis from the local plumb line with a theodolite. The first method was used routinely.

Compact strong sources were observed at the frequencies 22 and 36 GHz with coordinates known with precision better than $1''$ (Nesterov, 1985). The position of the antenna which gives the maximum registered power was found and small differences between the computed elevation and azimuth angles and the angles measured by sensors were determined. These differences were approximated as

$$\begin{aligned} \Delta A &= -a_1 \sin H \cos A + a_2 \sin H \sin A + a_3 \sin H + a_4 \cos H + a_5 \cos H \sin A + \\ & \quad a_6 \cos H \cos A + a_7 \\ \Delta H &= h_1 \sin A + h_2 \cos A + h_3 \sin H + h_4 \cos H + h_5 \end{aligned} \tag{1}$$

where A is azimuth, H is elevation. Coefficients a_i, h_j were found by solving the system of equations 1 for azimuth and elevation independently using LSQ. Parameters a_1, h_1, a_2, h_2 describe the inclination of the azimuthal axis.

The position of the azimuthal axis was episodically determined with a theodolite during 1966–1999. The theodolite was fixed on a moving part of the antenna's mounting and the antenna was repeatedly pointed to a sequence of different azimuths in increments $10°$–$20°$. Level readings of the vertical circle of the theodolite holding a fixed position of the tube were approximated to a sinusoid by LSQ.

Positions of both horizontal and azimuthal axis were also carefully measured with $2''$ precision during a special survey campaign in 1995 (Samoilenko, 1996). One of the conclusions of the surveying campaign was that *"a more detailed study of the complete dataset gives us grounds to believe that the azimuthal axis draws a cone in space and has smooth random wobbles when the antenna moves in azimuth. Nevertheless, the total effect does not exceed ±1 mm"*. We can consider this estimate as the upper limit of the short-term stability of the antenna's reference point.

The time series of the deviation of the azimuthal axis with respect to the local plumb line as a function of time is presented in figure 2. The inclination angle is increasing with a rate of $2''.6$ per year in the direction of azimuth 116°, and we believe the antenna is leaning like the tower of Pisa . We model the antenna's motion as a rotation with respect to the center of its gravity. Velocity of the antenna's reference point due to the Pisa-effect is -0.1 mm/year in the north direction and 0.2mm/year in the east direction.

Fig. 2: Deviation of azimuthal axis of the radiotelescope with respect to the local plumb line (in arc seconds) at different epochs.

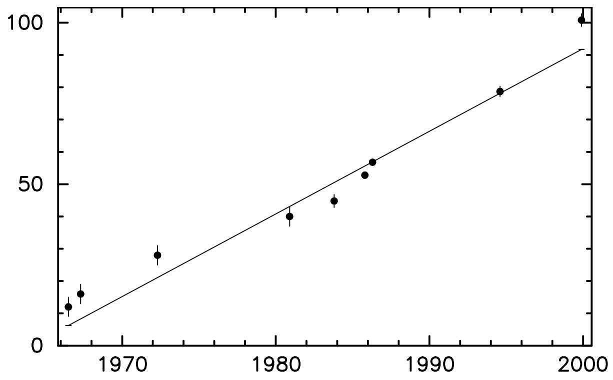

Evaluation of station performance

Performance of the station did not remain constant during the campaign of observations. It was noticed in 1995 that the estimates of the clock function showed random fluctuations on the level of 300–1000 psec, which is one order of magnitude larger than expected. It was found that the H-maser, which should generate a stable harmonic signal with frequency 5 MHz for all components of the data acquisition system, had unsatisfactory stability. Eventually, the old maser was replaced and a new maser started to operate on February 1, 1998. The estimates of the clock function using the old and new H-maser are shown in figure 3.

It was found that the model of estimation of clock function was not adequate for the processing of experiments when the stability the of H-maser was especially poor. Unaccounted variations of clocks resulted in spurious variation in the estimates of atmosphere path delay. The rate of changes of the estimates of the atmosphere path delay during two experiments 96MAR13XA and 97SEP03XA exceeded 150 psec/hour while even severe meteorological conditions do not cause variations in the path delay greater than 50 psec/hour. These two experiments were excluded from the final solution.

We investigated the amplitudes of the phase calibration signal injected into the feed horn and found a presence of coherent spurious signals, induced by others parts of equipment. The procedure of correction of phase calibration, described in (Petrov, 2000), was applied, but it resulted in only a marginal change in the station position estimates.

fig. 3: Estimates of the clock function during a 24-hours experiment (in psec)

a) Experiment 97MAY14XA b) Experiment 98AUG17XA

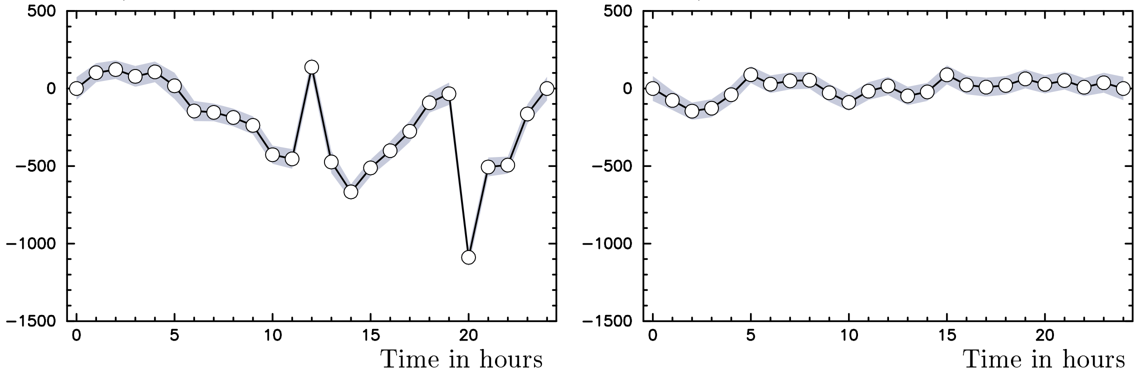

The position of the station Simeiz was estimated for each session independently in solution 2. Series plots of vertical, east and north station coordinates with respect to the position obtained in that solution are shown in figure 4. An error bar is the one-sigma formal uncertainty.

fig. 4: Evolution of topocentric coordinate of Simeiz (in mm)

a) Vertical component b) East component c) North component

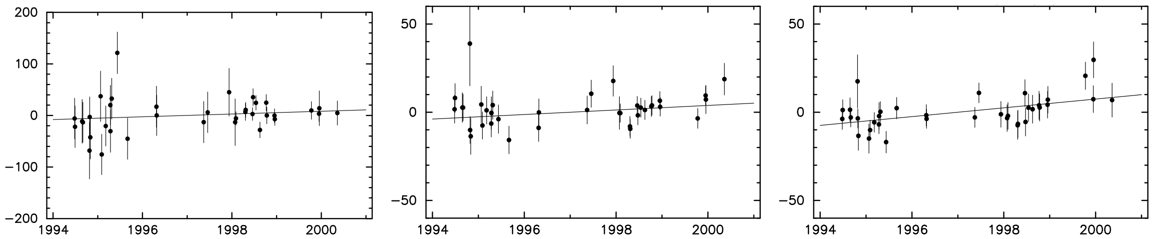

Vertical component:	rate = 2.4 ± 2.6 mm/yr	wrms = 27.0 mm	$\chi^2/\mathrm{ndg} = 6.5$
East component:	rate = 1.5 ± 0.6 mm/yr	wrms = 5.8 mm	$\chi^2/\mathrm{ndg} = 5.8$
North component:	rate = 2.6 ± 0.6 mm/yr	wrms = 5.2 mm	$\chi^2/\mathrm{ndg} = 4.5$

Figure 4 shows that the estimates of the station coordinates have scatter larger than predicted in accordance with the formal errors of the observations obtained on the basis of the signal to noise ratio of fringe phases and baseline-dependent variances. These variances were added quadratically to the raw formal uncertainties of the observables in order to keep the ratio of the weighted sum of the squares of the post-fit residuals to its mathematical expectation close to unity. The spread of the adjustments of station coordinates is larger for the first part of the dataset when the old H-maser was used, especially for the vertical coordinate.

The position of the station at the reference epoch 1997.0 and its rate of change were obtained by a weighted LSQ fit from the time series of the estimates. Correlations between the estimates at different epochs were neglected. A chi-square test was made in order to evaluate the correspondence of the linear parametric model of the station motion and the stochastic model which describes statistical characteristics of the noise. The ratio of the weighted sum of the squares of the postfit residuals to its mathematical expectation, denoted as χ^2/ndg, appears to be significantly higher than 1. This indicates the presence of excessive noise which our parametric and stochastic models do not properly take into account. A reweighting procedure was applied: the formal uncertainties of the station positions were modified by quadratically adding a variance v, such that: $\sigma_{ni}^2 = \sigma_{oi}^2 + v^2$ in order to make the ratio of the weighted sum of the squares of the postfit residuals to its mathematical expectation close to unity. Here the index $_o$ denotes the old formal error and the index $_n$ denotes the new formal error. Variance v is considered a constant before and after the H-maser replacement and it has a discontinuity at that moment. A pair of values of variances were found independently for each component of the coordinates. The algorithm used is described by Petrov (Petrov, 1995b). This caused some changes in the estimates of the station velocities and their formal uncertainties.

It was found that the poor performance of the H-maser affected the estimates of the vertical coordinates greater than the estimates of the horizontal coordinates. The horizontal components of position and velocity of the station Simeiz were treated as global parameters, while the vertical coordinate was estimated for each session independently in solution 3. Finally, the vector of the estimates of the station velocity was formed in the following procedure: a) the horizontal components are the estimates from solution 3; b) the vertical component of the velocity vector is obtained by adjusting the rate of the time series of the estimates from solution 3 with reweighting applied; c) the covariance matrix was scaled as $\mathrm{Cov}_n(x_i, x_j) = s_i s_j \,\mathrm{Cov}_o(x_i, x_j)$ where $s_k = \dfrac{\sigma_{nk}}{\sigma_{ok}}$. These manipulations enable us to obtain more reliable adjustments of the station position and velocity and the estimates of their accuracy.

Transformations of the velocity field

However, we should be aware that the position and velocity of a single station are senseless unless the coordinate frame has been defined. VLBI observables are invariant with respect to the group of 15-parametric linear transformations which include a rotation and translation of station positions and velocities, rotation of source positions, applies a shift and a linear drift to a series of Earth orientation parameters (Petrov, 1999). This means that the velocity field is defined only up to an arbitrary translation and rotation. Constraints which have been applied in solving equations of condition forced the obtained velocity field to have no net rotation and no net translation with respect to the a priori velocity field. In order to compare the catalogue of station positions and velocities with models and other catalogues a linear transformation which satisfies the explicitly specified boundary conditions should be applied.

We consider two problems. First, what is the residual velocity of the station Simeiz with respect to the Eurasian tectonic plate?

Nine permanent VLBI stations with a history of observations more than 3 years are located on the Eurasian plate: SIMEIZ, DSS65, EFLSBERG, MATERA, MEDICINA, NYALES20, ONSALA60, SESHAN25 and WETTZELL. In order to determine the residual velocity of each station with respect to the rigid motion of the plate, we first split the set of stations onto two groups: defining stations and free stations. Rigid motion means that the plate as a whole has a translational and rotational motion only. Defining stations are assumed to move in accordance with the motion of the plate, while free stations are assumed to have an arbitrary velocity with respect to the plate. Transformation of the velocity field is of the form

$$\vec{v}_n = \vec{v}_o + \vec{T} + \vec{\Omega} \times \vec{r} \tag{2}$$

where $\vec{v}_o$ is the old velocity vector, $\vec{T}$ is the vector of the translational velocity, $\vec{\Omega}$ is the vector of the angular velocity, $\vec{r}$ is the vector of the station position. This equation may be re-written in the form

$$\vec{v}_n = \vec{v}_o + \widehat{\mathcal{M}}\, \vec{s} \tag{3}$$

where

$$\widehat{\mathcal{M}} = \begin{pmatrix} 1 & 0 & 0 & 0 & r_3 & -r_2 \\ 0 & 1 & 0 & -r_3 & 0 & r_1 \\ 0 & 0 & 1 & r_2 & -r_1 & 0 \end{pmatrix} \qquad \vec{s} = \begin{pmatrix} T_1 \\ T_2 \\ T_3 \\ \Omega_1 \\ \Omega_2 \\ \Omega_3 \end{pmatrix} \tag{4}$$

Equation 3 is transformed to a local topocentric reference frame by multiplying it by the rotation matrix P:

$$\widehat{\mathcal{P}}_i \widehat{\mathcal{M}}_i\, \vec{s} = \vec{u}_i - \widehat{\mathcal{P}}_i\, \vec{v}_{oi} \tag{5}$$

where $\vec{u}$ is the vector of the station velocity in a topocentric reference frame after the transformation. We can find vector $\vec{s}$ in equation 5 if we define $\vec{u}_i$ according to the model of rigid motion. We set vector $\vec{u}_i = 0$ for the defining stations in our solution. Four stations, DSS65, EFLSBERG, NYALES20 and WETTZELL, were selected as defining, while the equations for the vertical component of stations DSS65, EFLSBERG, NYALES20 were down-weighted and therefore these stations were allowed to have an arbitrary vertical motion. Equations were solved by LSQ with a full weights matrix $\widehat{\mathcal{W}}$:

$$\widehat{\mathcal{W}} = \widehat{\mathcal{D}} \left(\widehat{\mathcal{P}}_a \operatorname{Cov}(v, v^\top)\, \widehat{\mathcal{P}}^\top_a + \widehat{\mathcal{A}} \right)^{-1} \tag{6}$$

where $\widehat{\mathcal{P}}_a$ is a block-diagonal matrix formed from matrices $\widehat{\mathcal{P}}_i$, $\widehat{\mathcal{A}}$ is a diagonal reweighting matrix with an additive correction to weights, $\widehat{\mathcal{D}}$ is a diagonal matrix which consist of elements 1 and $1 \cdot 10^{-5}$. The latter value effectively down-weights the equation. Values $(0.4\ \mathrm{mm/year})^2$ for both horizontal and vertical components of velocities were used in the matrix $\widehat{\mathcal{A}}$ in our solution.

Transformation 3 and the rotation to the local topocentric frame were applied to both defining and free stations. The covariance matrix was computed as:

$$\begin{aligned} \operatorname{Cov}(v_n, v_n^\top) &= \widehat{\mathcal{P}}_a \operatorname{Cov}(v_o, v_o^\top) \widehat{\mathcal{P}}^\top_a \; + \; \widehat{\mathcal{P}}_a \widehat{\mathcal{M}} \operatorname{Cov}(s, s^\top) \widehat{\mathcal{M}}^\top \widehat{\mathcal{P}}^\top_a \\ \operatorname{Cov}(v_n, v_n^\top) &= \widehat{\mathcal{P}}_a \operatorname{Cov}(v_o, v_o^\top) \widehat{\mathcal{P}}^\top_a \; + \; \widehat{\mathcal{P}}_a \widehat{\mathcal{M}} \operatorname{Cov}(s, s^\top) \widehat{\mathcal{M}}^\top \widehat{\mathcal{P}}^\top_a \; + \\ & \widehat{\mathcal{P}}_a \operatorname{Cov}(s, s^\top) \widehat{\mathcal{M}} \widehat{\mathcal{W}} \operatorname{Cov}(v_o, v_o^\top) \widehat{\mathcal{P}}^\top_a \; + \; \widehat{\mathcal{P}}_a \operatorname{Cov}(v_o, v_o^\top) \widehat{\mathcal{W}} \widehat{\mathcal{M}}^\top \operatorname{Cov}(s, s^\top) \widehat{\mathcal{P}}^\top_a \end{aligned} \tag{7}$$

The upper expression was used for the free stations and the lower expression was used for the defining stations. The latter expression takes into account statistical dependence of the old velocity $\vec{v}_o$ and the vector $\vec{s}$.

The field of residual horizontal velocities is shown in figure 5 and table 1.

Fig. 5: The field of residual horizontal velocities with respect to the Eurasian plate.

■ denotes a defining station
● denotes a free station

Tab. 1: Residual station velocities with respect to the Eurasian plate.

Station	Up (mm/yr)	East (mm/yr)	North (mm/yr)	Corr E-N	Hor. Rate (mm/yr)	Azimuth (Deg)	D
DSS65	2.1 ± 1.5	-0.1 ± 0.2	0.0 ± 0.1	0.86	0.1 ± 0.2	271°±51°	h
EFLSBERG	-0.5 ± 0.8	0.5 ± 0.3	-0.4 ± 0.2	0.03	0.7 ± 0.2	132°±22°	h
MATERA	1.1 ± 0.9	0.9 ± 0.4	4.9 ± 0.4	0.30	5.0 ± 0.5	11°± 5°	f
MEDICINA	-3.1 ± 0.8	1.7 ± 0.4	2.0 ± 0.4	0.11	2.6 ± 0.4	40°± 8°	f
NOTO	0.6 ± 1.0	-1.0 ± 0.5	5.0 ± 0.4	0.30	5.1 ± 0.4	349°± 6°	f
NYALES20	5.8 ± 1.5	0.0 ± 0.0	0.0 ± 0.0	-0.92	0.0 ± 0.0	350°±65°	h
ONSALA60	3.3 ± 0.6	-1.0 ± 0.4	-0.8 ± 0.4	-0.11	1.3 ± 0.3	229°±17°	f
WETTZELL	-0.0 ± 0.1	-0.3 ± 0.2	0.4 ± 0.2	-0.04	0.5 ± 0.2	322°±25°	hv
SIMEIZ	**2.7 ± 3.0**	**1.3 ± 0.7**	**2.5 ± 0.9**	**0.07**	**2.8 ± 0.9**	**27°±15°**	f

The last column contains status of the station: free (f), defining for horizontal motion (h), defining for both horizontal and vertical motion (hv).

The second problem is to define the position and velocity of the station Simeiz in some well known reference frame. Parameters of transformation 3 were found by minimizing differences in the positions and velocities of the primary stations with respect to the ITRF97 catalogues. Station positions and velocities in the ITRF97 catalogue were considered as exactly known while the estimates of the velocities obtained in solution 3 were treated as stochastic parameters with the covariance matrix produced in this solution. Elements of the covariance matrix of the velocity and position components of the station Simeiz were scaled as mentioned above. We obtained the following position of the station Simeiz at epoch 1997.0 and its rate of change in the ITRF97 system:

$$
\begin{aligned}
X &= 3785231.070 \pm 0.006 \text{ m} & \dot{X} &= 6.8 \cdot 10^{-10} \pm 0.3 \cdot 10^{-10} \text{ m/sec} \\
Y &= 2551207.415 \pm 0.004 \text{ m} & \dot{Y} &= 5.0 \cdot 10^{-10} \pm 0.4 \cdot 10^{-10} \text{ m/sec} \\
Z &= 4439796.360 \pm 0.008 \text{ m} & \dot{Z} &= 2.1 \cdot 10^{-10} \pm 0.8 \cdot 10^{-10} \text{ m/sec}
\end{aligned}
$$

Discussion of results and conclusion

The station Simeiz is located in 300 km from the edge of the Eurasian plate. Tectonic motion in the eastern Mediterranean is complicated as a result of interaction of the Eurasian, African and Arabian plates (Mueller and Kahle, 1993). The boundary of the tectonic plates is associated with the North Anatolian transform fault. The Anatolian block moves westward along the fault and in turn is pushed by the African and Arabian plates northwards, causing deformation in the southern part of the Eurasian plate. Obtained horizontal velocity with a rate of 2.8 ± 0.9 mm/year in the direction with azimuth 27° does not contradict this model.

We would like to emphasize that the residual velocities depend on the choice of the defining stations. The fact that there exists four stations with deviations from rigid motion less than the formal uncertainties of the estimates of their velocities indicates the validity of the assumption that the obtained velocities of VLBI stations satisfactory represent tectonic motion. Simulations showed that the velocity of the station Simeiz is relatively insensitive to variations in the velocities of the defining stations. Changing the velocities of the defining stations up to 3 formal uncertainties did not cause changes in the horizontal velocity of Simeiz greater than 0.9 of the reweighted formal error.

The Pisa effect contributes to the local velocity of the antenna's reference point at the level of 0.2 mm/year and this has been taken into account. The station foundation is laid on a solid rock and we do not expect considerable local motions. The position of the reference point of the antenna with respect to the local marks was determined with a precision of 1 mm in 1995 and it is planned to repeat these measurements in the future.

Acknowledgment

VLBI is possible only as a result of the coordinated efforts of many people. The authors would to like to thank D. Ivanov, A. Ipatov and S. Mardyshkin for maintenance of the receivers at the station, M. Sorgente for his efforts in correlation as well as the personnel at 126 other VLBI stations, correlators and analysis centers. We are grateful to L.I. Matveenko for useful discussions that resulted in improving this paper.

References

1. Bolotin, S., Gaiovitch, I., Khoda, et. al., GPS Observational Campaign in the Geodynamics Test Area "Simeiz-Katziveli": Data Processing and Results, *Kosmichna Nauka i Technologija, dodatok do zhurnalu*, 1995, **1**, p. 3.

2. Broderick, J.J., Vitkevich, V.V., Jauncey, D.L., et al., Observations of compact radio sources with a radio interferometer having a Green Bank — Crimea baseline, *Sov. Astron.*, 1970, **47**, p. 627.

3. Clark, T.A., Corey, B.E., Davis, J.L., et al., Precision geodesy using the MARK-III very long baseline interferometric systems, *IEEE Transactions. Geoscience and Remote Sensing*, 1985, **23**, p. 438–449.

4. Clark, T.A., Bosworth, J., Vandenberg, N., et al., Precision Measurements of the Location of the VLBI Station Simeiz, *Astron. Let.*, 1995, **21**, p. 116-117.

5. Hase, H. and Petrov, L., The First Campaign of Observations with the VLBI-Module of TIGO, *Proceedings of the 13th Working Meeting on European VLBI for Geodesy and Astrometry*, Schlüter, W. and Hase, H., Eds:, Wettzell: BKG, 1999, p. 19–24. (Web: `http://fw1.wettzell.ifag.de/euro13/postscript/hase1.ps.gz`)

6. Himwich E., Introduction to the Field System for Non-Users, *IVS 2000 General Meeting Proceedings* ed. by N. Vandenberg and K. Baver, 2000, p.86–90 (Web: `http://ivscc.gsfc.nasa.gov/publications/gm2000/himwich2`)

7. MacMillan, D. and Ma, C., Evaluation of very long baseline interferometry atmospheric modeling improvements, *Journ. Geophys. Res.*, **99**, N 1, 1994, pp.637–651.

8. Matveenko, L.I., Kardashev, A.C., Sholomitckij, G.B., On Radiointerferometer with a Large Base, *Izvestija vuzov. Radiofizika*, 1965, **8**, N4, p.651–654.

9. Matveenko, L.I. Kopelyanskii G.D., Shevchenko A.V., et al., Radiointerferometry observations on the Eastern hemisphere antennas, *Astron. Letters*, 1992, **18**, p.891.

10. Mueller, S. and Kahle, H-G., Crust-Mantle Evolution, Structure and Dynamics of the Mediterranean-Alpine Region, *Contribution of Space Geodesy to Geodynamics: Crustal dynamic*, Smith, D. and Tucotte, D., Eds, Geodynamics Series, **23**, Washington D.C.: AGU, 1993, p. 249–298.

11. Nesterov, N., Systematic errors of pointing the RT-22 radiotelescope, *Izvestija KrAO*, 1985, **73**, p. 189.

12. Petrov, L., Ivanov, D.V., Ipatov, A.V., et al., First results of determination of the position of station Simeiz from geodetic VLBI observations, *Proceedings of the XXVI Russian radioastronomical conference*, St.Petersburg, 1995, p. 230.

13. Petrov, L., Secondary data analysis of geodetic VLBI observations. III. Estimation of model's parameters, *Communications of the Institute of Applied Astronomy N76*, Institute of Applied Astronomy, 1995, St.Petersburg, p. 47.

14. Petrov, L., Absolute methods for determination of reference system from VLBI observations, *Proceedings of the 13th Working Meeting on European VLBI for Geodesy and Astrometry*, Schlüter, W. and Hase, H., Eds:, Wettzell, BKG, 1999, p. 138–143.
(Web: `http://fw1.wettzell.ifag.de/euro13/postscript/petrov2.ps.gz`)

15. Petrov, L., Instrumental errors of geodetic VLBI, *IVS 2000 General Meeting Proceedings* ed. by N. Vandenberg and K. Baver, 2000, p.230–235
(Web: `http://ivscc.gsfc.nasa.gov/publications/gm2000/petrov1`)

16. Pyne, T., Gwinn, C., Birkinshaw et al., Gravitational Radiation and Very Long Baseline Interferometry *ApJ*, 1996, **465**, p.566–577.

17. Ray, J., Corey, B., Current precision of VLBI multi-band delay observable, *Proceedings of the AGU Chapman conference on geodetic VLBI: Monitoring Global Change*, NOAA Technical Report NOS 137 NGS 49, Washington, D.C., 1991, pp.123–134.

18. Samoilenko, A., Local geodetic network at Simeiz geodynamics test area, *Preprint of the Main Astronomical Observatory*, Kiev, 1996, p. 37.

19. Sovers, O., Fanselow, J., Jacobs, C., Astrometry and geodesy with radio interferometry: experiments, models, results, *Reviews of Modern Physics*, 1998, **70**, p. 1393–1454.

20. Takahashi, F., Kondo, T., Takahashi, Y., et al., Very Long Baseline Interferometer, Ohmsha Ltd., 2000, 237 p.

21. Tatevian, S.K. and Shtirberg L.S., Collocation of different space geodesy technique at the Simeiz geodynamical observatory, *Proceedings of the International workshop on geodetic measurements by the collocation of space techniques on Earth (GEMSTONE)*, January 25-28, 1999, CRL, Tokyo, Japan, p. 45–49.

22. Walter, H.G. and Sovers, O.J., Astrometry of Fundamental Catalogues, Springer Verlag, 2000, 231 p.

23. Vandenberg, N., Eds:, *International VLBI Service for Geodesy and Astrometry — 1999 Annual report*, 1999, Greenbelt, USA, p. 308.
(Web: `http://ivscc.gsfc.nasa.gov/publications/ar1999/`)